

# Rethinking the Learning Paradigm for Facial Expression Recognition

Weijie Wang, Bo Li\*, Jiawen Zheng, Weizhi Nie, Hao Zhang, Jinwei Chen, Nicu Sebe *Senior Member, IEEE*, Bruno Lepri

**Abstract**—Due to the subjective crowdsourcing annotations and the inherent inter-class similarity of facial expressions, real-world Facial Expression Recognition (FER) datasets usually exhibit ambiguous annotation. To simplify the learning paradigm, most existing methods convert ambiguous annotation results into precise one-hot annotations and train FER models in an end-to-end supervised manner. In this paper, we rethink the existing training paradigm and propose that it is better to use weakly supervised strategies to train FER models with original ambiguous annotation. Specifically, we model FER as a Partial Label Learning (PLL) problem, which allows each training example to be labeled with an ambiguous candidate set. To better utilize representation learning to boost label disambiguation in PLL, we propose to use the Masked Image Modeling (MIM) strategy to learn the feature representation of facial expressions in a self-supervised manner. Then, these feature representations are used to query the probabilities of ambiguous label candidates, which are used as the ground truth in the PLL label disambiguation process. Extensive experiments on RAF-DB, FERPlus, and AffectNet demonstrate that the PLL learning paradigm substantially outperforms the current fully supervised state-of-the-art approaches in FER.

**Index Terms**—Facial expression recognition, Partial label learning, Deep learning.

## I. INTRODUCTION

Aiming at analyzing and understanding human emotions, Facial Expression Recognition (FER) [1]–[5] is an active field of research in computer vision with practical implications in social robotics, automatic driving, etc. FER leverages these multimedia elements (including images, videos, and audio) to interpret and understand human emotions by analyzing facial features, vocal tones, and other behavioral cues.

In recent years, FER has achieved impressive performance on laboratory-controlled datasets, such as CK+ [6], JAFFE [7] and RaFD [8], which are collected under ideal conditions and annotated by experts. Recently, with the demands of real-world applications, large-scale FER datasets in unconstrained environments, such as FERPlus [9], RAF-DB [10] and AffectNet [11], continue to emerge. However, collecting large-

Weijie Wang and Nicu Sebe are with the Department of Information Engineering and Computer Science, University of Trento, Trento 38123, Italy. E-mail: {weijie.wang, niculae.sebe}@unitn.it.

Weizhi Nie is with the School of Electrical and Information Engineering, Tianjin University, E-mail: weizhi.nie@tju.edu.cn

Bo Li, Hao Zhang, and Jinwei Chen are with vivo Mobile Communication Co., Ltd, China. E-mail: {libra, haozhang, 11112388}@vivo.com \*Corresponding author.

Jiawen Zheng is with ByteDance Inc, China. E-mail: zhengjiawen@bytedance.com

Bruno Lepri is with Fondazione Bruno Kessler, Italy. E-mail: lepri@fbk.eu  
Manuscript received April 19, 2021; revised August 16, 2021.

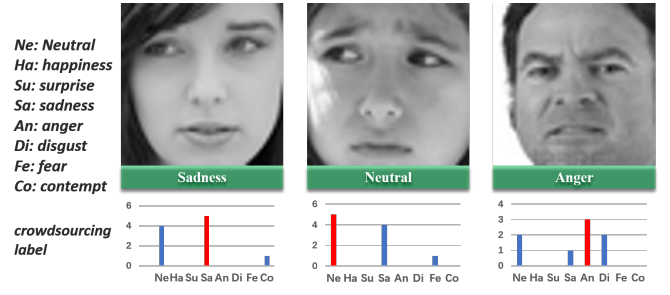


Fig. 1. These samples are from the FERPlus dataset, with the corresponding labels in green, which are obtained by voting on the results of the crowdsourcing annotations. This label conversion strategy can introduce artificial noise.

scale datasets with fully precise annotations is labor-intensive and challenging. Consequently, the crowdsourcing approach is commonly utilized for annotation. Due to the subjective perception of annotators and the inherent inter-class similarity of facial expressions, real-world FER datasets usually exhibit ambiguous annotation. To make it easier to use the crowdsourcing annotation results, most previous methods convert them into precise one-hot annotations by simply voting [9] or thresholding [10] and train FER models in an end-to-end supervised manner. However, these label conversion strategies do not always yield satisfactory results as shown in fig. 1. The performance of models supervised with such converted labels is inevitably impeded.

In this paper, we rethink the existing training paradigm and propose that it is better to use weakly supervised strategies to train FER models with original ambiguous annotation. Specifically, we model FER as a Partial Label Learning (PLL) problem, where each training instance is associated with a set of candidate labels among which exactly one is true, reducing the overhead of finding the exact label from ambiguous candidates [12].

The major challenge of PLL lies in the label disambiguation. Existing PLL methods [13]–[16] state that examples close to each other in the feature space will tend to share identical labels in the label space and their label disambiguation is based on this assumption. However, there is a contradiction here: the direct use of ambiguous annotations inevitably affects the quality of representation learning, which in turn hinders label disambiguation. Errors can accumulate severely, especially with the low-quality initial representations [17].

To mitigate the influence of ambiguous labels on feature learning, we propose to use unsupervised learning to obtain

the initial feature representation. Specifically, we propose to use the recently emerged Masked Image Modeling (MIM) to pre-train facial expression representation. MIM is mostly built upon the Vision Transformer (ViT), which suggests that self-supervised visual representations can be done by masking input image parts while requiring the target model to recover the missing contents. Facial expressions are high-level semantic information obtained from the combination of action units in multiple regions of the human face. Vision Transformer can model the relationship between action units with the global self-attention mechanism. MIM pre-training forces the ViT to learn the local facial action units and global facial structures in various expressions [18]. Then the pre-trained ViT is finetuned with an ambiguous label set in the PLL paradigm. Moreover, unlike other tasks, facial expression data exhibit high inter-class similarity, which makes label disambiguation more challenging.

In this paper, we propose to treat the label disambiguation process as querying the confidence of the correlation between each category label and features. Specifically, inspired by DETR [19], we propose a decoder-based label disambiguation module. We leverage learnable label embeddings as queries to obtain confidence in the correlation between features and the corresponding label via the cross-attention module in the Transformer decoder. Finally, we integrate the encoder of the ViT backbone, and the Transformer decoder-based label disambiguation module to build a fully transformer-based facial expression recognizer in the partial label learning paradigm. Our contributions are summarized as follows:

- We rethink the existing training paradigm of FER and propose to use weakly supervised strategies to train FER models with original ambiguous annotation. To the best of our knowledge, it is the first work that addresses the annotation ambiguity in FER with the Partial Label Learning (PLL) paradigm.
- We build a fully transformer-based facial expression recognizer, in which we explore the benefits of the facial expression representation based on MIM pre-train and the Transformer decoder-based label confidence queries for label disambiguation.
- Our method is extensively evaluated on large-scale real-world FER datasets. Experimental results show that our method consistently outperforms state-of-the-art FER methods. This convincingly shows the great potential of the Partial Label Learning (PLL) paradigm for real-world FER.

## II. RELATED WORK

### A. Facial Expression Recognition

Facial Expression Recognition (FER) [11], [20]–[22] aims to help computers understand human behavior and even interact with humans. FER can be mainly divided into traditional-based and deep learning-based methods. For the former, it mainly focuses on hand-designed texture-based feature extraction for in-the-lab FER datasets, on which the recognition accuracy is very high.

Since then, most studies tried to tackle the in-the-wild FER task. These large-scale datasets are collected in an unconstrained environment and annotated by crowdsourcing. Due to the subjective perception of annotators and the inherent inter-class similarity of facial expressions, real-world FER datasets usually exhibit ambiguous annotation. Previous methods [23]–[27] convert the annotation results into precise one-hot annotations by simply voting [9] or thresholding [10] and train FER models in an end-to-end supervised manner. However, these label conversion strategies do not always yield satisfactory results as shown in fig. 1. The performance of models supervised with such converted labels is inevitably impeded. In recent years, several attempts try to address the ambiguity problem in FER. SCN [20] and RUL [28] relabel noisy samples automatically by learning clean samples to suppress uncertainty from noise labels. DMUE [29] proposes a method of latent label distribution mining and an inter-sample uncertainty assessment, which aims to solve the problem of label ambiguity. However, they either require the noise rate for better noise filtering or rely on sophisticated architectures, which limit their generalization to in-the-wild situations.

Recently, some researchers move from fully-supervised learning (SL) to semi-supervised learning (SSL). Ada-CM [30] proposes an SSL method by adaptive learning confidence margins to utilize all unlabeled samples during training time, which represents a new idea to solve FER tasks by making use of additional unlabeled data. In this paper, we rethink the existing training paradigm and propose that it is better to use weakly supervised strategies to train FER models with original ambiguous annotation. As fig. 1 shows, in-the-wild facial expressions often include compound emotions or even mixture ones. Thus, for these samples with uncertainty, it is natural to have multiple annotated candidates. Consequently, for the first time, a new Partial Label Learning (PLL) paradigm is proposed to address the annotation ambiguity in FER.

### B. Partial Label Learning

Partial Label Learning (PLL) is an important category of weakly supervised learning methods in which each object has multiple candidate labels, but only one of them is the ground-truth label. It is mainly divided into average-based and identification-based methods. The most intuitive solution is average-based methods, which generally consider each label to be equally important during training time, and make predictions by averaging the output of all candidate labels [31], [32]. Others [33], [34] utilize a parametric model to maximize the average scores of candidate labels minus that of non-candidate labels. The identification-based methods normally maximize the output of the most likely candidate labels to disambiguate the ground-truth label. Some typical methods mainly include maximum margin criterion [35], graph-based [36]. With the development of deep learning, more network structures [37], [38] emerge, which rely on the output of the model itself to disambiguate the candidate label sets. Some researchers argue [39]–[41] that data points closer in feature space are more likely to be classified as the same label, which relies on a good feature representation. PICO [42] reconciles PLL-based label disambiguation and feature representation based

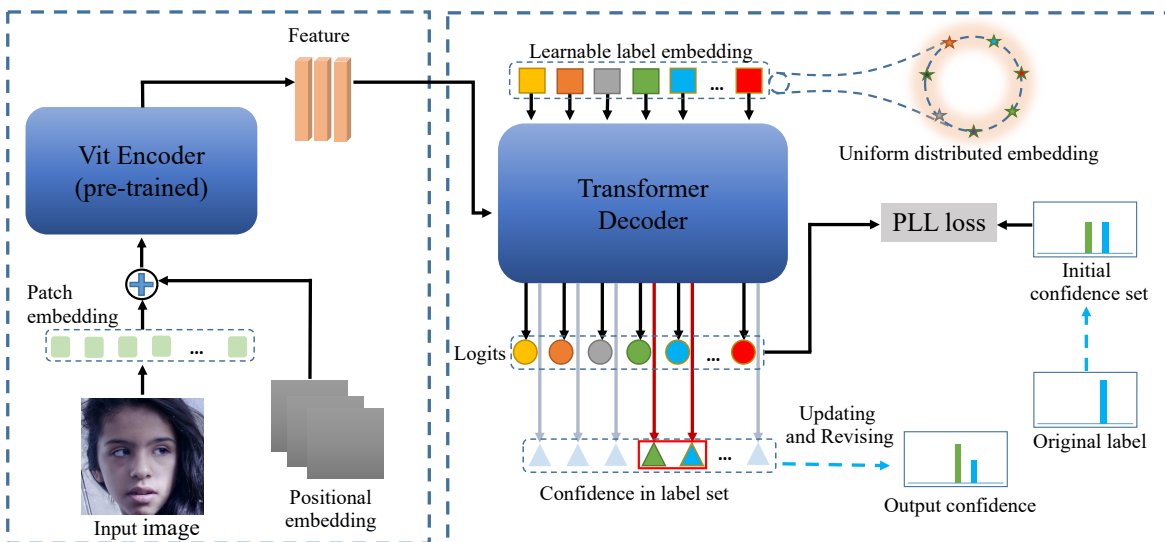


Fig. 2. The overview of our framework. In the left part, we use the pre-trained ViT encoder as our backbone for the feature representation of the 2D image, In the right part, we input the obtained feature from the left part to the transformer decoder with learnable label embedding. After that, we revise  $(i-1)_{th}$  confidence and update it to get  $i_{th}$  confidence. Finally, the loss is computed between logits and  $i_{th}$  confidence.

on contrastive learning. However, elaborately designed data augmentation is essential due to its sensitivity to positive sample selection. Another drawback of contrastive learning in FER is that the high inter-class similarity of facial expressions makes it hard to obtain robust feature representations.

### C. Masked Image Modeling

Inspired by Masked Language Modeling (MLM), Masked Image Modeling (MIM) has become a popular self-supervised method. iGPT [43] predicts unknown pixels by operating on known pixel sequences. ViT [44] predicts masked patch prediction by employing a self-supervised approach. Moreover, iBOT [45] achieves excellent performance through siamese networks. However, these methods have the assumption of image semantic consistency. The ability of BEiT [46] to predict discrete tokens depends on the pre-trained model VQVAE [47] that it relies on. As an extension of the ViT work, the main aim of SimMIM [48] is to predict pixels. Unlike the previously mentioned approaches, MAE [49] proposes an encoder-decoder architecture that uses the decoder for the MIM task. Differently, Maskfeat [50] adopts hog descriptor as a prediction target rather than pixels. Currently, the potential benefits of MIM for enhancing PLL performance have not been well studied.

## III. METHOD

In this section, we introduce a fully transformer-based facial expression recognizer with a new partial label learning paradigm, which mainly consists of a process of robust learning representation and label disambiguation. Fig. 2 shows an overview of our framework. Generally, given an in-the-wild FER dataset  $\mathcal{D}(\mathcal{X}, \mathcal{Y})$ , each sample  $x_i$  is assigned to one of the  $K$  deterministic categories, denoted as  $y_i \in \{y_1, y_2, \dots, y_k\}$ ,

### A. Partial Label Learning (PLL)

Partial label learning (PLL) aims to predict a true label of the input using a mapping of the classification function. It can tolerate more uncertainty from the label space, and gradually eliminate it in a weakly supervised way during the training. In PLL, each sample in the partially labeled dataset  $\tilde{\mathcal{D}}$  is represented by  $(x_i, Y_i)$ , where  $Y_i$  is a set of candidate labels corresponding to  $x_i$ .

**Label set construction.** The first step of using PLL is to construct a label set,  $Y_i = \{y_1, y_2, \dots, y_k\}$ , as the input. Given this label set, PLL would then recognize the potential (unseen) true label  $y_i$  of each sample  $x_i$  from  $Y_i$  by training a classifier, which computes the probability of each class in the candidate label set. Here we adopt the method in [51] to determine the potential ambiguous samples. For the ambiguous samples, we consider binary values and assign 1 to the components in  $Y_i$  that correspond to the top- $k$  predictions and assign 0 to the rest. We normalize each label set  $Y_i$  to obtain a confidence vector  $C_i = \{c_1, c_2, \dots, c_k\}$ , with all values summing up to 1.

In the training stage, a classifier  $\zeta : \mathcal{X} \rightarrow \mathcal{C}^k$  is trained to update the confidence vector  $c_i$ . We expect the  $c_i$  to concentrate most of the probability density on the true label  $y_i$  of the sample  $x_i$ . We use the categorical cross-entropy loss to constrain it as follows:

$$\mathcal{L}_{pll}(x_i, C_i) = \sum_{j=1}^k -C_i \log(\zeta^i(x_i)), \text{ s.t. } \sum_{j=1}^k c_{i,j} = 1, \quad (1)$$

where  $j$  denotes the index of confidence vector  $C_i$ .  $\zeta^i(\cdot)$  is the softmax layer of the model. In the following, we continue to describe the two key modules in our framework: model pre-training and label disambiguation.

### B. Model Pre-training

An important assumption of PLL is that samples close to each other in the sample space are more likely to share an

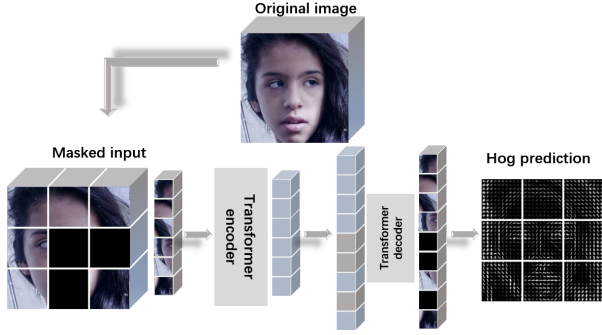


Fig. 3. We adopt masked image modeling (MIM) for pre-training, which involves predicting the hog descriptor (HOG) with the randomly masked input. After obtaining the pre-trained model, we fine-tune it for the FER task within our partial label learning paradigm.

identical label in the label space, which indicates that a good feature representation is important [14], [34], [41]. Based on this assumption, we choose to pre-train the model to achieve a better representation. Since the model is easily misled by ambiguous labels, fully-supervised pre-training may not be a good choice. Therefore, we adopt masked image modeling (MIM) [49], a self-supervised model, which avoids the use of potentially ambiguous labels. The structure of MIM is illustrated in fig. 3. Specifically, in the encoder part, we adopt the encoder of ViT [44], which only acts on the visible and unmasked patches. For the decoder, we adopt hog descriptors as the prediction target of the decoder rather than pixel values [49]. In this way, we expect MIM to learn the local facial action units and global facial structures in various facial expressions.

In FER, focusing on such unit-level information is more meaningful than focusing on pixel-level information. Indeed, pixel-level information can often be distorted by details such as high-frequency nuances, lighting conditions, and fluctuations in contrast. In the pre-training stage, we only keep the encoder for feature extraction and discard the decoder.

### C. Label Disambiguation

The label disambiguation with the transformer decoder includes the label embedding regularization module and the confidence revision module. An input image  $x$  is fed into the pre-trained encoder to get visual tokens  $\mathcal{F}^{HW \times d}$ , where  $HW$  denotes the number of visual tokens and  $d$  denotes the feature dimension of the hidden state. We initialize the query embedding  $\mathcal{Q}^{k \times d}$ , where  $k$  denotes the number of classes. In the fine-tuning stage, the transformer decoder updates  $\mathcal{Q}^{k \times d}$  according to visual tokens, with  $\mathcal{Q}^{k \times d}$  reflecting the correlation of category-related features. Inspired by [52], [53], we link the category-related features to the learnable query embedding  $\mathcal{Q}^{k \times d}$  and predict the confidence sector  $C_i$  of the sample by their correspondence. Specifically,  $C_i$  is obtained by inputting the logits from the last layer of the transformer decoder to the sigmoid function. However, differently by [52], [53], (1) our method is designed for PLL and focuses on disambiguation by query to finally find the unique correct label with the highest confidence for each instance. (2) Besides querying

the classification logits, we also query the label confidence. (3) To mitigate the problem of imbalance distribution in the FER dataset, we design a special regularization for label embedding.

1) *Label Embedding Regularization.*: It is worth noting that in addition to the annotation ambiguity, these FER datasets also commonly exhibit imbalance distribution. In the training stage, it makes the model more biased towards majority classes, resulting in an uneven distribution of the feature space, and degrading model performance by classifying minority classes as head classes. In our work, we draw inspiration from [54] and aim to achieve a uniform distribution of the query embedding over a hypersphere to mitigate the negative effects of class imbalance. Specifically, we compute a uniform loss for query embedding to pull the distance between different classes on the hypersphere. We compute the optimal positions for different classes of query embedding  $\{t_i\}_{i=1}^K$  before training and optimize it using the following (eq. (2)):

$$\mathcal{L}_{uniform}(\{t_i\}_{i=1}^K) = \frac{1}{K} \sum_{i=1}^K \log \sum_{j=1}^K e^{t_i^T \cdot t_j / \tau}, \quad (2)$$

where  $\tau > 0$  is a temperature hyperparameter, and  $K$  denotes the number of classes in FER dataset.

2) *Revision Confidence.*: As previously mentioned, the robust representation in the feature space enhances PLL's ability to disambiguate in the label space. For samples with ambiguous labels in the dataset, we initially set the candidate label set  $Y$  with a uniform distribution, represented by  $C_i = \frac{1}{|Y_i|} Y_i$ . During the update process, we continuously revise the confidence score  $C_i$  for each batch using the following (eq. (3)):

$$\begin{pmatrix} id_1 : v_1 \\ id_2 : v_2 \end{pmatrix} = Top_k[\varphi * C_{i-1}], k = 2, \quad (3)$$

where  $\varphi = sigmoid(\sigma_{logits})$  is the response of sigmoid layer, and  $\sigma_{logits}$  is the output of the transformer decoder. After that, we compute the top-2 metrics of the  $(C_{i-1} * \varphi)$  for updating confidence vector  $C_i$  as the (eq. (4)):

$$C_i = \begin{cases} C_{i-1} & \Delta v \leq threshold \\ C_{i-1}[id_1] = 1 & else \end{cases}, \quad (4)$$

where  $\Delta v = |v_1 - v_2|$ , the threshold  $\in [0, 1)$ . When  $\Delta v > threshold$ ,  $C_i$  is a one-hot vector, where only the 1-th entry is 1. We treat it as the level of uncertainty and represent it with the top-2 rank label in the candidate label set. algorithm 1 is the pseudo-code of our method, which would converge to a stable status along the training iterations. We specifically choose top-2, because we notice that the accuracy of most samples located in top-2 reaches 95%.

## IV. EXPERIMENTS

In this section, we describe the FER datasets in section IV-A, implementation details in section IV-B, pre-training, and fine-tuning details in section IV-C, comparison with Fer methods in section IV-D, ablation studies in section IV-E and visualization results in section IV-F.

**Algorithm 1** Pseudo-code of our method

---

**Require:** *Model*  $f$ : Pre-trained model  $f$ ;  
*Epoch*  $T_{max}$ : Number of total epochs;  
*Iteration*  $I_{max}$ : Number of total iterations;  
*query embedding*: query  $Q$  ;  
*Dataset*  $\tilde{D}$  : partially labeled training set  $\tilde{D} = \{(x_i, Y_i)\}_{i=1}^n$  ;

**Ensure:**  
 $C_i = \frac{1}{|Y_i|} Y_i (i \in Y)$ , initialize the confidence vector  $C_i$ ;  
**for**  $i = 1, 2, \dots, T_{max}$  **do**  
  **Shuffle**  $\tilde{D} = \{(x_i, Y_i)\}_{i=1}^n$  ;  
  **for**  $j = 1, 2, \dots, I_{max}$  **do**  
    **fetch** mini-batch  $\tilde{D}_j$  from  $\tilde{D}$ ;  
    **calculate** Uniform distribution for query by eq. (2);  
    **revise** confidence vector  $C_i$  by eq. (3) and eq. (4);  
    **calculate** PLL loss by eq. (1)  
    **update** Network parameter of  $f$  by eq. (1);  
  **end for**  
**end for**

---

To evaluate our proposed framework, we compare it with a baseline and other related methods including **fully-supervised learning**: PSR [25], DDA [26], SCN [20], SCAN [27], DMUE [29], RUL [28], DACL [55], MA-Net [56], MVT [57], VTFF [58], EAC [59], and TRANSFER [60], LA-Net [61]; and **partial label learning**: RC [62], LW [38], PICO [42], and CRPLL [63].

## A. Datasets.

**RAF-DB** [64] contains around 30K diverse facial images with single or compound expressions labeled by 40 trained annotators via crowdsourcing. In our experiments, we use 12271 images for training and 3068 images for testing. **FERPlus** [9] is an extended dataset of the standard emotion FER dataset with 28709 training, 3589 validation, and 3589 test images. It provides a set of new labels for each image labeled by 10 human annotators. According to previous work, we just use the train part and test part. **AffectNet** [11] is one of the most challenging FER datasets with manually labeled 440k images. As per prior research, we divide it into AffectNet-7 and AffectNet-8, with the latter having one more expression of contempt and 3667 training and 500 test images more compared to the former.

## B. Baseline and Experiment Setup.

We adopt ViT-B/16 [44] pre-trained on Imagenet-1K as our baseline. For fairness, we keep the same parameters as our fine-tuning part in all settings, which will be described later. In terms of SL methods, we adopt their optimal settings to make fair comparisons. For data preprocessing, we keep all the images with the size of  $224 \times 224$  and use MobileFacenet [66] to obtain aligned face regions for RAF-DB and FERPlus. For AffectNet, alignment was obtained via the landmarks provided in the data. In the pre-training part, we use four Tesla V100 GPUs to pre-train the ViT for 600 epochs with batch size 192 and learning rate  $2e-4$ . We set the mask ratio of Maskfeat to

0.4. In the fine-tuning part, we use only two Tesla V100 GPUs. We utilize the AdamW optimizer, setting the batch size to 320 and the initial learning rate to  $1e-4$  with the weight decay of  $5e-2$ . The pre-training and fine-tuning protocol that we use is based on [50].

## C. Details for pre-training and fine-tuning

table II and table III summarize the pre-training configurations of different pre-trained methods. table IV shows the fine-tuning configurations on the FER dataset. We use three FER datasets to pre-train the encoder part and adopt 2 transformer blocks in the decoder part.

## D. Comparison with the SOTA FER Methods

We conduct extensive comparisons with the SOTA FER methods on RAF-DB, FERPlus, AffectNet-7, and AffectNet-8 respectively. Specifically, we compare with **ResNet18-based** methods, which are pre-trained on the face recognition dataset MS-Celeb-1M [67]: SAN [20], DMUE [29], RUL [28], DACL [55], MA-Net [56], DDA [26], and EAC [59]; with **ResNet50-based** methods: SCAN [27]. In addition, we also compare with **transformer-based** approaches such as MVT [57], VTFF [58], and TRANSFER [60]. Finally, we also compare with PSR [25] using **VGG-16**. We list all the comparison results in table I. We achieve the highest performance on all datasets as shown in table I. From the results, our method outperforms all current SOTA methods for FER, including ResNet-based and transformer-based methods. Specifically, we exceed the baseline [44] by 3.69%, 2.93%, 2.5%, 2.78% accuracy on RAF-DB, FERPlus, AffectNet-7, AffectNet-8.

1) *Comparison with SL methods*: Considering the latest SL methods, we surpass EAC [59] by 2.06% and 1.79% on RAF-DB and AffectNet-7 respectively, PSR [25] by 1.36% on FERPlus, and DMUE [29] by 1.28% on AffectNet-8. These experimental results show the effectiveness of our proposed method in the FER task and demonstrate that converting ambiguous annotation results into one-hot labels using fully-supervised learning is not ideal. Compared to PLL, these CNN-based SL methods are misled by the ambiguous labels in the label space, which hinders the performance of the model. Furthermore, the transformer-based SL method suffers from the same problems. Although MVT [57] employs ViT as the backbone, it does not utilize unsupervised pre-training. Nevertheless, it remains susceptible to ambiguous labels in the label space, resulting in potential impacts on feature learning quality, which is consistent with the hypothesis proposed in [68]. The same problem exists with VTFF [58] and TRANSFER [60].

2) *Comparison with PLL methods*: We also compare with several representative PLL methods: RC [62], LW [38], PICO [42], and CRPLL [63]. For a fair comparison, we use their optimal experimental settings. The results in table I are our implementation based on their open-source codes. The general PLL method for label disambiguation, e.g. RC and LW, relies on the robustness of the features, and from the results, for the FER task, RC, LW, and CRPLL are



TABLE I  
COMPARISON WITH THE STATE-OF-THE-ART RESULTS ON THE RAF-DB, FERPLUS, AFFECTNET7, AND AFFECTNET8 DATASETS. ACCURACY (ACC.(%)) IS REPORTED ON THE TEST DATASET.

Method	Backbone	RAF-DB	FERPlus	AffectNet7	AffectNet8
PSR [25]	VGG-16	88.98	89.75	63.77	60.68
DDA [26]	ResNet-18	86.90	-	62.34	-
SCN [20]	ResNet-18	87.03	88.01	63.40	60.23
SCAN [27]	ResNet-50	89.02	89.42	65.14	61.73
DMUE [29]	ResNet-18	88.76	88.64	-	62.84
RUL [28]	ResNet-18	88.98	88.75	61.43	-
DACL [55]	ResNet-18	87.78	88.39	65.20	60.75
MA-Net [56]	ResNet-18	88.40	-	64.53	60.96
MVT [57]	DeiT-S/16	88.62	89.22	64.57	61.40
VTFE [58]	ResNet-18+ViT-B/32	88.14	88.81	64.80	61.85
EAC [59]	ResNet-18	89.99	89.64	65.32	-
TransFER [60]	CNN+ViT	90.91	89.76	66.23	-
LA-Net [65]	ResNet-50	91.56	67.60	-	-
RC [62]	ResNet-18	88.92	88.53	64.87	61.63
LW [38]	ResNet-18	88.70	88.10	64.53	61.46
PICO [42]	ResNet-18	88.53	87.93	64.35	61.38
CRPLL [63]	ResNet-18	88.47	88.01	64.32	61.37
Baseline [44]	ViT-B/16	88.36	88.18	64.61	61.34
Ours	ViT-B/16	<b>92.05</b>	<b>91.11</b>	<b>67.11</b>	<b>64.12</b>

TABLE II  
PRE-TRAINING SETTING, PART I.

configs	MAE	MaskFeat
Base Learning Rate	1.5e-4	2.5e-5
Batch_Size	1024(4096)	1024(2048)
Warm Up	40	40
Weight_Decay	0.05	0.05
-Norm_Pix_Loss	True	False
Mask-Ratio	85%(75%)	85%(40%)
Epoch	600	600
Optimizer	AdamW	AdamW
Optimizer Momentum	0.9,0.95	0.9,0.999
Mask_Patch	16	16

TABLE III  
PRE-TRAINING SETTING, PART II.

configs	MoCo	SimMIM
Base Learning Rate	0.03	1.5e-4(1e-4)
Batch_Size	256	1024(2048)
Warm Up	0	40
Weight_Decay	1e-4	0.05
-Norm_Pix_Loss	False	False
Mask-Ratio	0	75%(60%)
Epoch	200	800
Optimizer	SGD	AdamW
Optimizer Momentum	0.9	0.9,0.95
Mask_Patch	0	16(32)

TABLE IV  
FINE-TUNING SETTING OF MASKFEAT ON FER DATASETS.

configs	RAF-DB	FERPlus	AffectNet-7/8
Base Learning Rate	1e-4	1e-4	1e-4
Batch_Size	320	320	320
Weight_Decay	5e-2	5e-2	5e-2
Mask-Ratio	40%	40%	40%
Epoch	100	100	25
Optimizer	AdamW	AdamW	AdamW
OptimizerMomentum	0.9,0.95	0.9,0.95	0.9,0.95

misled by ambiguous labels in the label space, which affects disambiguation due to the lack of robust facial expression feature representation. In addition, it is worth noting the result of PICO demonstrates that contrastive-based partial label learning does not apply to the FER task. As mentioned before, the contrastive-based approach is sensitive to data augmentation. Unlike objects, facial expressions have high inter-class similarities, which consist of five fixed facial action units; whereas typical data augmentation usually works on the lighting and contrast variation of the image, which only leads to extra redundant information in the FER task, and, sometimes, even to performance degradation.

E. Ablation Study

In this part, we conducted extensive ablation experiments, including: the effectiveness of PLL section IV-E1, the effectiveness of Pre-training section IV-E2, the feature-level effects of pre-trained SL, SSL section IV-E3, the confidence-level performance section IV-E4, the decoder and key modules section IV-E5, the ablation for threshold of revision confidence section IV-E6, the influence of  $K$  section IV-E7, and the ablation for temperature  $\tau$  section IV-E8.

TABLE V  
COMPARING SOFTMAX AND VANILLA PLL WITH DIFFERENT PRE-TRAINING MANNERS ON FER WITHOUT DISAMBIGUATION MODULE. “-PR” INDICATES PRE-TRAINING.

Method	RAF-DB	FERPlus	AffectNet-7
ResNet-18 + Softmax	86.54	87.37	63.86
ResNet-18 + PLL	88.67	88.40	64.49
Maskfeat-PR + Softmax	87.85	87.92	64.31
Maskfeat-PR + PLL	<b>90.35</b>	<b>90.24</b>	<b>66.12</b>

1) *Effectiveness of PLL Paradigm:* To validate the PLL paradigm, we solely utilize the ResNet-18 model pre-trained

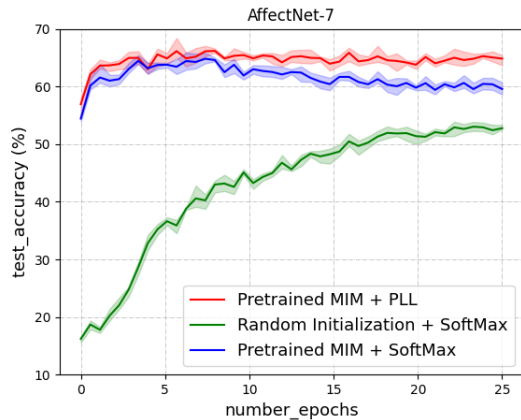


Fig. 4. Test accuracy during fine-tuning on AffectNet-7.

TABLE VI  
THE IMPACT OF PRE-TRAINING (PR).

Method	RAF	FER	Aff-7	Aff-8
Ours w/o PR	90.81	89.63	65.23	62.45
Ours	<b>92.05</b>	<b>91.11</b>	<b>67.11</b>	<b>64.12</b>

on the FER dataset MS-Celeb-1M [67]. We directly compare the traditional Softmax loss with the vanilla PLL loss, employing only (eq. (1)) without additional modules. The outcomes are reported in table V and fig. 4. (1) PLL loss consistently surpasses the Softmax loss, enhancing recognition accuracy by 2.13% on RAF-DB, 1.03% on FERPlus, and 0.63% on AffectNet-7. Thus, we experimentally verify that a good performance can be attained using ResNet-18 with the vanilla PLL loss. (2) As evident from fig. 4, during the initial training phases, pre-training establishes a solid foundation for feature initialization. However, as training advances, supervised learning gradually adjusts to ambiguous labels, making it sensitive to ambiguities within the label space, thus leading to performance degradation. In contrast, PLL exhibits greater resilience to the disruptive effects of ambiguous labels.

2) *Effectiveness of Pre-training:* As shown in table VI, we test the entire pipeline without using pre-training. Compared to “w/o PR”, pre-training has a significant performance gain. In this case, the robust features provided by pre-training further enhance the disambiguation ability of the PLL paradigm, even for vanilla PLL.

3) *Feature-level Effects of Pre-trained SL, SSL:* In contrast to supervised learning (SL), self-supervised learning (SSL) pre-training emerges as the optimal strategy for acquiring these resilient features in the FER task. In addition to employing ResNet-18 for SL pre-training, we also compare various other SSL pre-training methods (MoCo [69], SimMIM [48], MAE [49]) as presented in table VII. As previously highlighted, intuitively, the significance of unit-level information (e.g. eyes, nose, and mouth corners) surpasses that of pixel-level details (high-frequency nuances, lighting, contrast), because the structure of the face consists of multiple facial action units. This demonstrates that combining Maskfeat [50]

TABLE VII  
THE IMPACT OF MODEL ARCHITECTURE USED FOR PRE-TRAINING. NO DISAMBIGUATION MODULE IS USED.

Method	RAF	FER	Aff-7
ResNet-18	88.67	88.40	64.49
MoCo	88.59	88.14	63.98
MIM (SimMIM)	89.60	89.78	65.34
MIM (MAE)	89.99	89.70	65.79
MIM (Maskfeat)	<b>90.35</b>	<b>90.24</b>	<b>66.12</b>

with PLL forms a more effective self-supervised learning paradigm for FER. Notably, MoCo [69] demonstrates instead diminished effectiveness in FER due to its sensitivity to data augmentation, which has minimal influence on the facial structural components affected by variations in contrast and illumination within expression data.

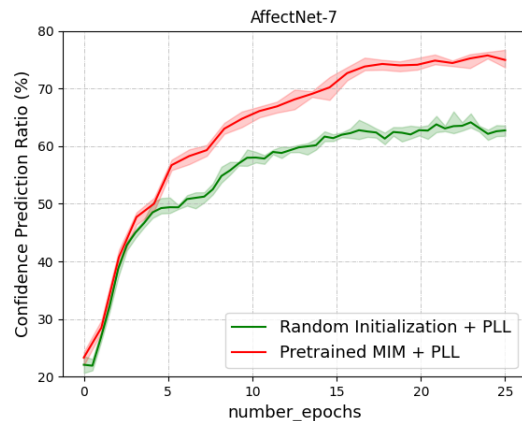


Fig. 5. The confidence correctness ratio of relabeled data on AffectNet-7.

4) *Confidence-level performance:* To intuitively observe and analyze the performance of PLL in terms of confidence, we artificially re-label and test 2k samples in the AffectNet-7 (the ratio of ambiguous labels is the highest in the FER dataset), and count the confidence ratio of these samples, as shown in fig. 5, compared to “Random init. + PLL”, the combination of features from “PLL” and “Pretrained” confers a greater capacity to resolve ambiguities. We argue that within this process, “PLL” plays a more pivotal role in terms of label disambiguation, yet its potential is fully harnessed when integrated with “Pretrained”.

5) *Evaluation of Decoder and key modules:* To evaluate the effectiveness of the transformer decoder and other key modules, we conduct an ablation study on RAF-DB and FERPlus as shown in table VIII. From the results, based on the PLL paradigm, the transformer decoder improves accuracy by 0.94% on RAF-DB and 0.55% on AffectNet7. The results show that it uses the cross-attention module to obtain the correlation of features and category labels via learnable label embedding, which in turn provides a more adequate foundation for the PLL disambiguation. As for the label uniform embedding module,  $\mathcal{L}_{uniform}$  alleviates the influence of imbalanced FER data classes by distributing

TABLE VIII  
THE IMPACT OF DECODER,  $\mathcal{L}_{uniform}$ , AND REVISION CONFIDENCE IN OUR DISAMBIGUATION MODULE.

Decoder	$\mathcal{L}_{uniform}$	Re-conf	RAF	Aff-7
✗	✗	✗	90.35	66.12
✓	✗	✗	91.29	66.67
✓	✓	✗	91.64	66.90
✓	✗	✓	91.89	66.93
✓	✓	✓	<b>92.05</b>	<b>67.11</b>

query embedding uniformly over the hypersphere. As for the revision confidence module, the revision confidence strategy can further facilitate the ability of PLL to disambiguate in the label space. This module enhances performance as an auxiliary module of disambiguation.

6) *Ablation for Threshold of Revision Confidence*: The revision confidence module relies on the output of the transformer decoder. In addition, the disambiguation ability of PLL is determined by setting a threshold for the uncertainty of the candidate set. We aim to find and revise the sample, whose confidence is less than the threshold. To evaluate the influence of different thresholds for disambiguation. We conduct an ablation study as fig. 6 and fig. 7 show.

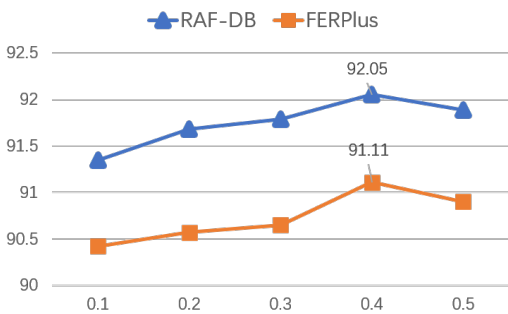


Fig. 6. The accuracy (%) with different thresholds on RAF-DB and FERPlus.

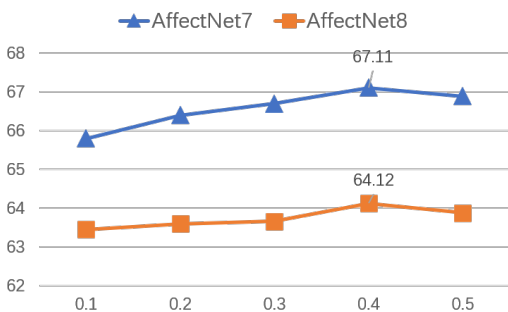


Fig. 7. The accuracy (%) with a different thresholds on AffectNet7 and AffectNet8.

7) *Influence of parameter K*: We conducted the influence of K in different settings. It is somewhat sensitive, and we have set k=2 for optimal performance. After conducting additional experiments, we observed that in 95% of cases, a true label is included for k=2, and this increases to 99% for k=3. In terms of performance, on the RAF-DB dataset, the recognition rates

are 92.35% for k=2, 91.94% for k=3, and 90.01% for k=4. It is evident that k is a bit sensitive to different settings, which is possibly due to the trade-off between increasing the possibility of including potential ground truth labels and the simultaneous increase in uncertainty and noise. Consequently, as k increases, the performance gradually declines.

8) *Ablation for Temperature Hyperparameter  $\tau$  and Calculation of the Confusion Matrix*: To correct the effects of unbalanced data classes, we propose  $\mathcal{L}_{uniform}$ , whose aim is to distribute the query embedding uniformly over the hypersphere to help the decoder better find the correlation between features and category labels. Inspired by [70], a small temperature coefficient is beneficial to distinguish the embedding of one category from the embedding of other categories. To verify its validity, we conducted an ablation study, as table IX shows.

TABLE IX  
THE ACCURACY (%) WITH DIFFERENT  $\tau > 0$  ON RAF-DB AND FERPLUS.

$\tau > 0$	0.001	0.005	0.01
RAF-DB	<b>92.35</b>	91.78	91.52
FERPlus	<b>91.41</b>	90.67	90.18

To demonstrate the validity of  $\mathcal{L}_{uniform}$  more intuitively, we calculated the confusion matrix for each category and calculated overall We show the results for the RAF-DB and FERPlus confusion matrix with respect to  $\mathcal{L}_{uniform}$  in fig. 8, fig. 9, respectively.

From the experimental results, the temperature hyperparameter  $\tau$  reaches the best performance at equal to 0.001, which demonstrates smaller temperature coefficients lead to a more uniform embedding space for query embedding, specifically in that the different classes of query embeddings on the hypersphere move away from each other.

From the confusion matrix on RAF-DB and FERPlus, we improve average accuracy on RAF-DB and FERPlus by 1.4%, 5.37%. In the head class, such as the "HAPPY" in RAF-DB, more test samples are classified to the tail class after using the  $\mathcal{L}_{uniform}$  constraint, which is beneficial to side effects of class imbalance and helps to eliminate bias to head class in the PLL disambiguation process; for FERPlus, the average accuracy improvement is relatively large, since its test samples are in the tail class, such as contempt, with only 15 images, which is an order of magnitude difference compared to the head class. When calculating the average accuracy, the improvement in accuracy in the tail class contributes significantly to the overall average precision.

F. Visualization of PLL disambiguation

To illustrate the disambiguation process of PLL more visually, we show the more visualization results of PLL disambiguation on RAF-DB, FERPlus, and AffectNet7 in fig. 10, fig. 11, and fig. 12, respectively.

G. Time/Memory Consumption of Proposed Method

We trained 600 epochs using 4 32GB Tesla V100s, requiring 3 days for pre-training, which takes longer and relatively



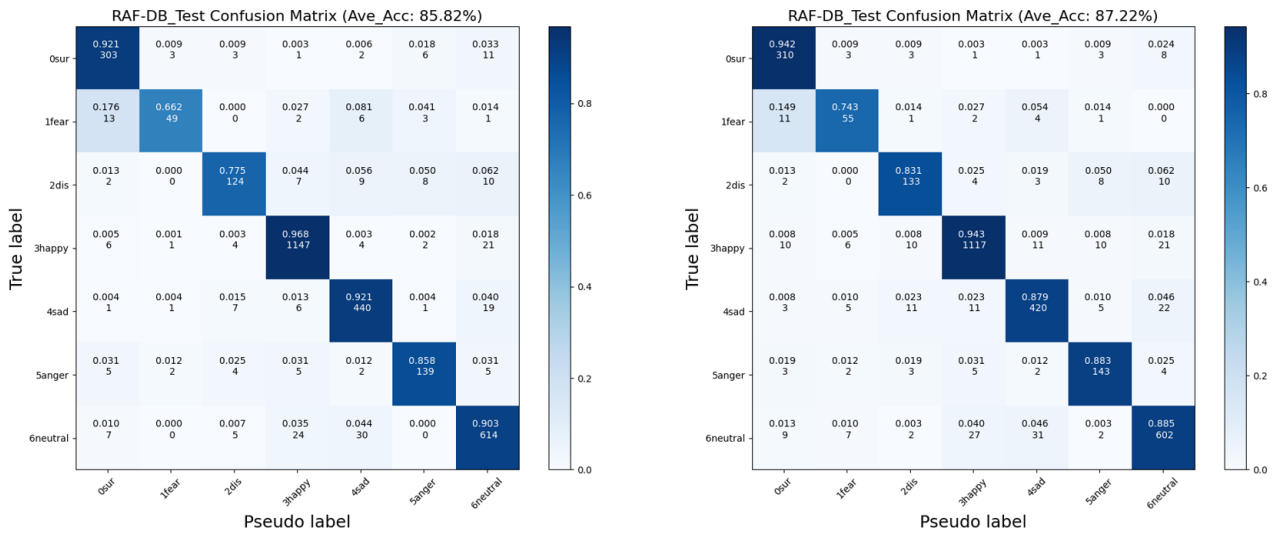


Fig. 8. The confusion matrix of the RAF-DB. Left part without  $\mathcal{L}_{uniform}$ , right part with  $\mathcal{L}_{uniform}$ .

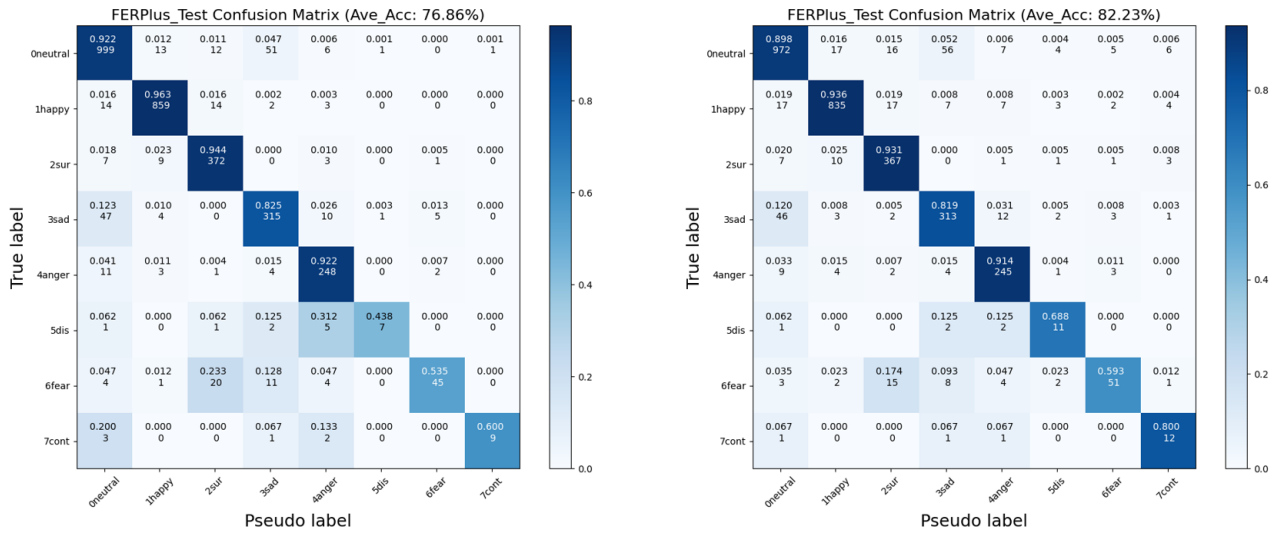


Fig. 9. The confusion matrix of the FERPlus. Left part without  $\mathcal{L}_{uniform}$ , right part with  $\mathcal{L}_{uniform}$ .

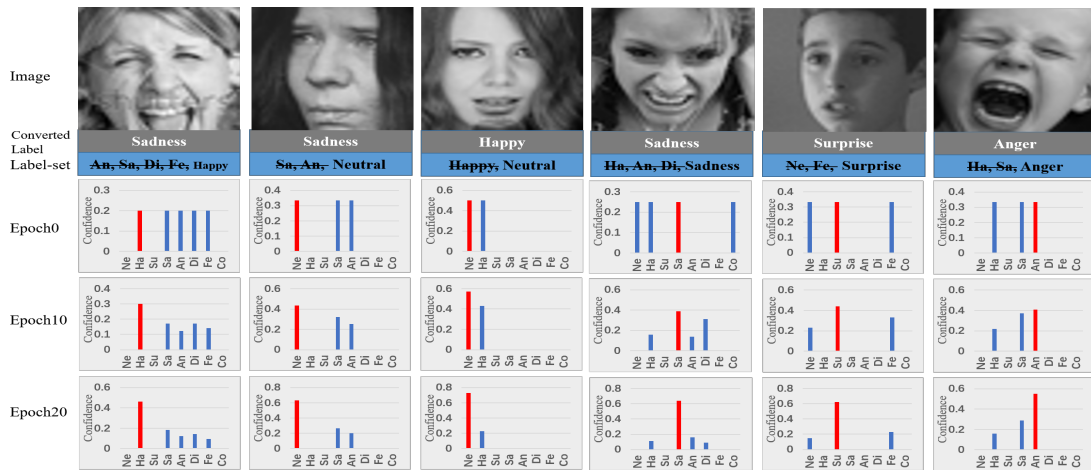


Fig. 10. The grey part of the figure shows the GT labels corresponding to the samples in FERPlus; the blue part shows the candidate set we constructed for the samples, where the strikethroughs mark the results of PLL disambiguation for error removal. The predicted labels are consistent with our intuition.

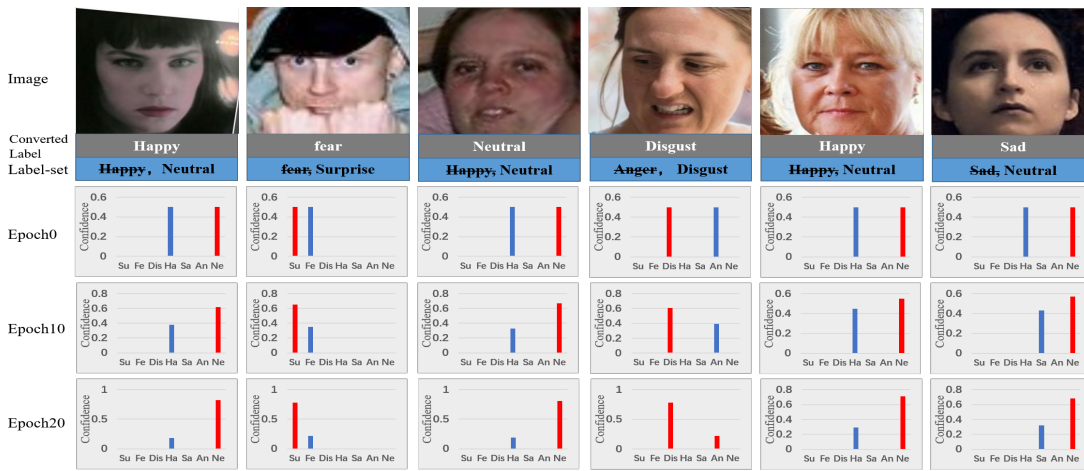


Fig. 11. The grey part of the figure shows the converted label, equivalent to GT, which is selected by the annotators from the crowdsourcing results in FERPlus. The blue part shows the candidate set we constructed for the samples corresponding to the converted(GT) labels, where the strikethroughs mark the results of PLL disambiguation for error removal. The predicted labels are consistent with our intuition.

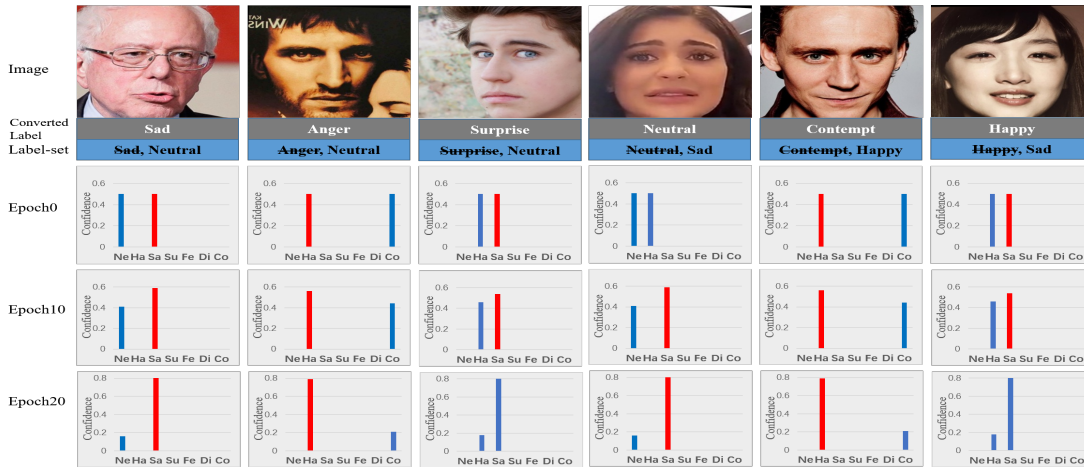


Fig. 12. The grey part of the figure shows the converted label, equivalent to GT, which is selected by the annotators from the crowdsourcing results in FERPlus. The blue part shows the candidate set we constructed for the samples corresponding to the converted(GT) labels, where the strikethroughs mark the results of PLL disambiguation for error removal. The predicted labels are consistent with our intuition.

more memory resources. The related pre-trained checkpoint will be released to help with FER downstream tasks. As for fine-tuning, we do an ablation on RAF-DB with batch size=72/128/256 and it takes around 1.43/1.2/1.18 hours and around 11/16/30 GB of memory, which is similar to DMUE [29])/MA-NET [56]/EAC [59]. However, we use similar resources to achieve better performance.

### V. CONCLUSION

In this paper, we rethink the existing training paradigm and propose that it is better to use weakly supervised strategies to train FER models with original ambiguous annotation. To solve the subjective crowdsourcing annotation and the inherent inter-class similarity of facial expressions, we model FER as a partial label learning (PLL) problem, which allows each training example to be labeled with an ambiguous candidate set. Specifically, we use the Masked Image Modeling (MIM) strategy to learn the feature representation of facial expressions in a self-supervised manner, even in the presence of ambiguous

annotations. To bridge the gap between the enriched feature representation and the partial labels, we introduce an adaptive transformer decoder module. This module is specifically designed to interpret the complex, high-dimensional features extracted by the MIM strategy. It dynamically adjusts its focus on the ambiguous candidate label sets, employing a soft attention mechanism to weigh the probabilities of each candidate being the true label. Extensive experiments show the effectiveness of our method. Our extensive experiments, conducted on several benchmark datasets for FER, underscore the superior performance of our proposed method over existing approaches. These results validate our hypothesis that modeling FER as a PLL problem and addressing it with a combination of MIM and transformer-based decoding is a potent strategy for enhancing the performance of FER systems. In conclusion, our findings suggest that weakly supervised strategies, augmented by self-supervised feature learning and transformer-based decoding, hold great promise for advancing the state-of-the-art in facial expression recognition.

## REFERENCES

- [1] S. Li and W. Deng, "Deep facial expression recognition: A survey," *IEEE Transactions on Affective Computing*, vol. 13, no. 3, pp. 1195–1215, 2022.
- [2] A. V. Savchenko, L. V. Savchenko, and I. Makarov, "Classifying emotions and engagement in online learning based on a single facial expression recognition neural network," *IEEE Transactions on Affective Computing*, vol. 13, no. 4, pp. 2132–2143, 2022.
- [3] Y. Li, J. Wei, Y. Liu, J. Kauttonen, and G. Zhao, "Deep learning for micro-expression recognition: A survey," *IEEE Transactions on Affective Computing*, vol. 13, no. 4, pp. 2028–2046, 2022.
- [4] P. Sarkar and A. Etemad, "Self-supervised ecg representation learning for emotion recognition," *IEEE Transactions on Affective Computing*, vol. 13, no. 3, pp. 1541–1554, 2022.
- [5] H.-X. Xie, L. Lo, H.-H. Shuai, and W.-H. Cheng, "An overview of facial micro-expression analysis: Data, methodology and challenge," *IEEE Transactions on Affective Computing*, vol. 14, no. 3, pp. 1857–1875, 2023.
- [6] P. Lucey, J. F. Cohn, T. Kanade, J. Saragih, Z. Ambadar, and I. Matthews, "The extended cohn-kanade dataset (ck+): A complete dataset for action unit and emotion-specified expression," in *CVPRw*, 2010.
- [7] M. Lyons, S. Akamatsu, and M. Kamachi, "Coding facial expressions with gabor wavelets," in *Proceedings Third IEEE international conference on automatic face and gesture recognition*, 1998, pp. 200–205.
- [8] O. Langner, R. Dotsch, G. Bijlstra, D. H. Wigboldus, S. T. Hawk, and A. Van Knippenberg, "Presentation and validation of the radboud faces database," *Cognition and Emotion*, 2010.
- [9] E. Barsoum, C. Zhang, C. Canton Ferrer, and Z. Zhang, "Training deep networks for facial expression recognition with crowd-sourced label distribution," in *ICMI*, 2016.
- [10] S. Li, W. Deng, and J. Du, "Reliable crowdsourcing and deep locality-preserving learning for expression recognition in the wild," in *CVPR*, 2017.
- [11] A. Mollahosseini, B. Hassani, and M. H. Mahoor, "Affectnet: A database for facial expression, valence, and arousal computing in the wild," *IEEE Transactions on Affective Computing*, 2017.
- [12] J. Lv, M. Xu, L. Feng, G. Niu, X. Geng, and M. Sugiyama, "Progressive identification of true labels for partial-label learning," in *ICML*, 2020.
- [13] H. Wang, R. Xiao, Y. Li, L. Feng, G. Niu, G. Chen, and J. Zhao, "Pico: Contrastive label disambiguation for partial label learning," *CoRR*, vol. abs/2201.08984, 2022. [Online]. Available: <https://arxiv.org/abs/2201.08984>
- [14] L. Liu and T. G. Dietterich, "A conditional multinomial mixture model for superset label learning," in *NeurIPS*, 2012.
- [15] M. Zhang, B. Zhou, and X. Liu, "Partial label learning via feature-aware disambiguation," in *Proceedings of the 22nd ACM SIGKDD International Conference on Knowledge Discovery and Data Mining, San Francisco, CA, USA, August 13-17, 2016*, B. Krishnapuram, M. Shah, A. J. Smola, C. C. Aggarwal, D. Shen, and R. Rastogi, Eds. ACM, 2016, pp. 1335–1344. [Online]. Available: <https://doi.org/10.1145/2939672.2939788>
- [16] G. Lyu, S. Feng, T. Wang, C. Lang, and Y. Li, "GM-PLL: graph matching based partial label learning," *IEEE Transactions Knowledge and Data Engineering*, vol. 33, no. 2, pp. 521–535, 2021. [Online]. Available: <https://doi.org/10.1109/TKDE.2019.2933837>
- [17] D. Wu, D. Wang, and M. Zhang, "Revisiting consistency regularization for deep partial label learning," in *ICML*, 2022.
- [18] K. He, X. Chen, S. Xie, Y. Li, P. Dollár, and R. Girshick, "Masked autoencoders are scalable vision learners," in *Proceedings of the IEEE/CVF Conference on Computer Vision and Pattern Recognition (CVPR)*, June 2022, pp. 16 000–16 009.
- [19] N. Carion, F. Massa, G. Synnaeve, N. Usunier, A. Kirillov, and S. Zagoruyko, "End-to-end object detection with transformers," in *Computer Vision - ECCV 2020 - 16th European Conference, Glasgow, UK, August 23-28, 2020, Proceedings, Part I*, ser. Lecture Notes in Computer Science, A. Vedaldi, H. Bischof, T. Brox, and J. Frahm, Eds., vol. 12346. Springer, 2020, pp. 213–229. [Online]. Available: [https://doi.org/10.1007/978-3-030-58452-8\\_13](https://doi.org/10.1007/978-3-030-58452-8_13)
- [20] K. Wang, X. Peng, J. Yang, S. Lu, and Y. Qiao, "Suppressing uncertainties for large-scale facial expression recognition," in *CVPR*, 2020.
- [21] P. C. Ng and S. Henikoff, "Sift: Predicting amino acid changes that affect protein function," *Nucleic Acids Research*, 2003.
- [22] S. Albanie, A. Nagrani, A. Vedaldi, and A. Zisserman, "Emotion recognition in speech using cross-modal transfer in the wild," in *ACMMM*, 2018.
- [23] C. Wang, S. Wang, and G. Liang, "Identity- and pose-robust facial expression recognition through adversarial feature learning," in *ACM MM*, 2019.
- [24] H. Yang, U. A. Ciftci, and L. Yin, "Facial expression recognition by de-expression residue learning," in *CVPR*, 2018.
- [25] T.-H. Vo, G.-S. Lee, H.-J. Yang, and S.-H. Kim, "Pyramid with super resolution for in-the-wild facial expression recognition," *IEEE Access*, 2020.
- [26] A. H. Farzaneh and X. Qi, "Discriminant distribution-agnostic loss for facial expression recognition in the wild," in *CVPRw*, 2020.
- [27] D. Gera and S. Balasubramanian, "Landmark guidance independent spatio-channel attention and complementary context information based facial expression recognition," *Pattern Recognition Letters*, 2021.
- [28] Y. Zhang, C. Wang, and W. Deng, "Relative uncertainty learning for facial expression recognition," in *NeurIPS*, 2021.
- [29] J. She, Y. Hu, H. Shi, J. Wang, Q. Shen, and T. Mei, "Dive into ambiguity: latent distribution mining and pairwise uncertainty estimation for facial expression recognition," in *CVPR*, 2021.
- [30] H. Li, N. Wang, X. Yang, X. Wang, and X. Gao, "Towards semi-supervised deep facial expression recognition with an adaptive confidence margin," in *CVPR*, 2022.
- [31] E. Hüllermeier and J. Beringer, "Learning from ambiguously labeled examples," *Intelligent Data Analysis*, 2006.
- [32] M.-L. Zhang and F. Yu, "Solving the partial label learning problem: An instance-based approach," in *IJCAI*, 2015.
- [33] T. Cour, B. Sapp, and B. Taskar, "Learning from partial labels," *Journal of Machine Learning Research*, 2011.
- [34] M.-L. Zhang, B.-B. Zhou, and X.-Y. Liu, "Partial label learning via feature-aware disambiguation," in *KDD*, 2016.
- [35] F. Yu and M.-L. Zhang, "Maximum margin partial label learning," in *ACML*, 2016.
- [36] D.-B. Wang, M.-L. Zhang, and L. Li, "Adaptive graph guided disambiguation for partial label learning," *IEEE Transactions on Pattern Analysis and Machine Intelligence*, 2021.
- [37] L. Feng and B. An, "Partial label learning with self-guided retraining," in *AAAI*, 2019.
- [38] H. Wen, J. Cui, H. Hang, J. Liu, Y. Wang, and Z. Lin, "Leveraged weighted loss for partial label learning," in *ICML*, 2021.
- [39] L. Liu and T. Dietterich, "A conditional multinomial mixture model for superset label learning," in *NeurIPS*, 2012.
- [40] Y. Zhang, X. Zhang, J. Li, R. Qiu, H. Xu, and Q. Tian, "Semi-supervised contrastive learning with similarity co-calibration," *IEEE Transactions on Multimedia*, 2022.
- [41] G. Lyu, S. Feng, T. Wang, C. Lang, and Y. Li, "Gm-pll: graph matching based partial label learning," *IEEE Transactions on Knowledge and Data Engineering*, vol. 33, no. 2, pp. 521–535, 2019.
- [42] H. Wang, R. Xiao, Y. Li, L. Feng, G. Niu, G. Chen, and J. Zhao, "Pico: Contrastive label disambiguation for partial label learning," in *ICLR*, 2022.
- [43] M. Chen, A. Radford, R. Child, J. Wu, H. Jun, D. Luan, and I. Sutskever, "Generative pretraining from pixels," in *ICML*, 2020.
- [44] A. Dosovitskiy, L. Beyer, A. Kolesnikov, D. Weissenborn, X. Zhai, T. Unterthiner, M. Dehghani, M. Minderer, G. Heigold, S. Gelly *et al.*, "An image is worth 16x16 words: Transformers for image recognition at scale," *arXiv preprint arXiv:2010.11929*, 2020.
- [45] J. Zhou, C. Wei, H. Wang, W. Shen, C. Xie, A. Yuille, and T. Kong, "Image bert pre-training with online tokenizer," in *ICLR*, 2022.
- [46] H. Bao, L. Dong, and F. Wei, "Beit: Bert pre-training of image transformers," in *ICLR*, 2022.
- [47] A. Van Den Oord, O. Vinyals *et al.*, "Neural discrete representation learning," in *NeurIPS*, 2017.
- [48] Z. Xie, Z. Zhang, Y. Cao, Y. Lin, J. Bao, Z. Yao, Q. Dai, and H. Hu, "Simmm: A simple framework for masked image modeling," in *CVPR*, 2022.
- [49] K. He, X. Chen, S. Xie, Y. Li, P. Dollár, and R. Girshick, "Masked autoencoders are scalable vision learners," in *CVPR*, 2022.
- [50] C. Wei, H. Fan, S. Xie, C.-Y. Wu, A. Yuille, and C. Feichtenhofer, "Masked feature prediction for self-supervised visual pre-training," in *CVPR*, 2022.
- [51] J. Zheng, B. Li, S. Zhang, S. Wu, L. Cao, and S. Ding, "Attack can benefit: An adversarial approach to recognizing facial expressions under noisy annotations," in *Proceedings of the AAAI Conference on Artificial Intelligence*, 2023, pp. 3660–3668.
- [52] N. Carion, F. Massa, G. Synnaeve, N. Usunier, A. Kirillov, and S. Zagoruyko, "End-to-end object detection with transformers," in *ECCV*, 2020.

- [53] S. Liu, L. Zhang, X. Yang, H. Su, and J. Zhu, "Query2label: A simple transformer way to multi-label classification," *arXiv preprint arXiv:2107.10834*, 2021.
- [54] T. Wang and P. Isola, "Understanding contrastive representation learning through alignment and uniformity on the hypersphere," in *ICML*, 2020.
- [55] A. H. Farzaneh and X. Qi, "Facial expression recognition in the wild via deep attentive center loss," in *WACV*, 2021.
- [56] Z. Zhao, Q. Liu, and S. Wang, "Learning deep global multi-scale and local attention features for facial expression recognition in the wild," *IEEE Transactions on Image Processing*, 2021.
- [57] H. Li, M. Sui, F. Zhao, Z. Zha, and F. Wu, "Mvt: mask vision transformer for facial expression recognition in the wild," *arXiv preprint arXiv:2106.04520*, 2021.
- [58] F. Ma, B. Sun, and S. Li, "Facial expression recognition with visual transformers and attentional selective fusion," *IEEE Transactions on Affective Computing*, 2021.
- [59] Y. Zhang, C. Wang, X. Ling, and W. Deng, "Learn from all: Erasing attention consistency for noisy label facial expression recognition," in *ECCV*, 2022.
- [60] F. Xue, Q. Wang, and G. Guo, "Transfer: Learning relation-aware facial expression representations with transformers," 2021.
- [61] Z. Wu and J. Cui, "La-net: Landmark-aware learning for reliable facial expression recognition under label noise," 2023.
- [62] L. Feng, J. Lv, B. Han, M. Xu, G. Niu, X. Geng, B. An, and M. Sugiyama, "Provably consistent partial-label learning," in *NeurIPS*, 2020.
- [63] D.-D. Wu, D.-B. Wang, and M.-L. Zhang, "Revisiting consistency regularization for deep partial label learning," in *International Conference on Machine Learning*. PMLR, 2022, pp. 24 212–24 225.
- [64] S. Li and W. Deng, "Reliable crowdsourcing and deep locality-preserving learning for unconstrained facial expression recognition," *IEEE Transactions on Image Processing*, vol. 28, no. 1, pp. 356–370, 2019.
- [65] Z. Wu and J. Cui, "La-net: Landmark-aware learning for reliable facial expression recognition under label noise," in *Proceedings of the IEEE/CVF International Conference on Computer Vision*, 2023, pp. 20 698–20 707.
- [66] S. Chen, Y. Liu, X. Gao, and Z. Han, "Mobilefacenets: Efficient cnns for accurate real-time face verification on mobile devices," in *CCBR*, 2018.
- [67] Y. Guo, L. Zhang, Y. Hu, X. He, and J. Gao, "Ms-celeb-1m: A dataset and benchmark for large-scale face recognition," in *ECCV*, 2016.
- [68] H. Liu, J. Z. HaoChen, A. Gaidon, and T. Ma, "Self-supervised learning is more robust to dataset imbalance," in *NeurIPS*, 2021.
- [69] K. He, H. Fan, Y. Wu, S. Xie, and R. Girshick, "Momentum contrast for unsupervised visual representation learning," in *CVPR*, 2020.
- [70] F. Wang and H. Liu, "Understanding the behaviour of contrastive loss," in *CVPR*, 2021.